Merging of momentum-space monopoles by controlling Zeeman field: From cubic-Dirac to triple-Weyl fermion systems

Motohiko Ezawa

Merging of momentum-space monopoles by controlling Zeeman field: From cubic-Dirac to triple-Weyl fermion systems

Motohiko Ezawa

Department of Applied Physics, University of Tokyo, Hongo 7-3-1, 113-8656, Japan

We analyze a generalized Dirac system, where the dispersion along the k_x and k_y axes is N-th power and linear along the k_z axis. In the presence of the Zeeman field, there emerge N monopole-antimonopole pairs by controlling it beyond a certain critical one. As the direction of the Zeeman field is rotated toward the z axis, monopoles move to the north pole while antimonopoles move to the south pole. When the Zeeman field becomes parallel to the z axis, they merge into one monopole or one antimonopole whose monopole charge is $\pm N$. The resultant system is a multiple-Weyl semimetal. Characteristic properties of such a system are that the anomalous Hall effect and the chiral anomaly are enhanced by N times and that N Fermi arcs appear. These phenomena will be observed experimentally in the cubic-Dirac and triple-Weyl fermion systems ($N = 3$).

Introduction: Topological objects in the momentum space play intriguing roles in condensed matter physics[1–4]. Examples are monopoles, skyrmions and merons. They have fascinating properties not shared by those in the real space, since they are purely static because of the absence of the kinetic energy. For instance, a monopole carrying a large magnetic charge cannot exist in the real space due to a large Coulomb repulsion but can in the momentum space. It is an interesting problem if we may generate N monopole-antimonopole pairs and successively make them merged into one monopole-antimonopole pair each of which carries monopole charge $\pm N$ just by controlling an external parameter.

Weyl semimetal is characterized by the monopole charge in the momentum space[5]. The characteristic features are the emergence of the anomalous Hall conductance[3,6,7], the chiral anomaly[8–12] and the Fermi arc[3,13,14]. It is possible to generate Weyl semimetals from Dirac semimetals by applying magnetic field[15,16]. This scenario of creating Weyl fermions has already been experimentally observed in GdPtBi[17,18], NdPtBi[18], Na$_3$ Bi[19] and Cd$_3$As$_2$[20–22]. Double- and triple-Weyl semimetals are generalization of Weyl semimetals, where the monopole charges are 2 and 3, respectively[23–30]. On the other hand, quadratic- and cubic-Dirac insulators have been proposed based on the symmetry considerations[24]. The dispersion is parabolic or cubic along the k_x and k_y directions, while it is linear along the k_z direction. Very recently, it is shown that the cubic Dirac semimetals would be materialized in quasi-one-dimensional transition-metal monochalcogenides by first-principles calculations[31].

In this paper we propose a simple model realizing a merging process of monopoles in the momentum space. It is a generalized Dirac system, where the dispersion along the k_x and k_y axes is N-th power and is linear along the k_z axis. Let us introduce the Zeeman field. Unless its direction is not along the z axis, there emerge N pairs of Weyl and anti-Weyl fermions beyond a certain critical value of the field. As the direction approaches the z axis, these Weyl fermions with the positive (negative) monopole charge move to the north (south) pole. When the Zeeman field becomes parallel to the z axis, they merge into one multiple-Weyl point whose monopole charge is $\pm N$. We show in such a system that the anomalous Hall effect is enhanced by N times, and furthermore that N Fermi arcs emerge.

Model Hamiltonian: The Zeeman term is induced by magnetization or external magnetic field. For the sake of clarity, first we introduce solely the magnetization. We investigate the Hamiltonian in the momentum space (k_x, k_y, k_z) given by

$$H = \tau_z \left[t a^N \left(k_+^N \sigma_- + k_-^N \sigma_+ \right) + t_z a_z k_z \sigma_z \right] + m\tau_x + \mathbf{h} \cdot \sigma,$$
(1)

where N is an arbitrary natural number; $k_\pm = k_x \pm i k_y$; t, t_z are constants of energy dimension; a, a_z are constants of length dimension; m is the mass parameter taken in energy dimension ($m > 0$); σ and τ are the Pauli matrices describing the spin and pseudospin degrees of freedom, respectively; $\sigma_\pm = \sigma_x \pm i\sigma_y$; $\mathbf{h} \cdot \sigma$ is the Zeeman term with $\mathbf{h}$ the Zeeman field. For simplicity we set $t = t_z = 1$ in what follows. They can be easily recovered since they appear always in pairs with a and a_z. The quadratic and cubic Dirac fermion systems are described by choosing $N = 2$ and 3 in the Hamiltonian (1), respectively.

Merging of N Weyl points: When $\mathbf{h} = \mathbf{0}$, the Hamiltonian describes an insulator with massive Dirac electrons whose dispersion is N-th power along the k_x and k_y directions and linear along the k_z direction: See Fig.1(a). Without loss of generality we can choose $\mathbf{h} = h(\sin\theta, 0, \cos\theta)$ and $h > 0$. The Hamiltonian (1) yields the energy spectrum $E_{\chi\eta} = \chi\sqrt{F + 2\eta h\sqrt{G}}$ with $\chi = \pm 1$, $\eta = \pm 1$, and

$$F = (ak)^{2N} + h^2 + m^2 + a_z^2 k_z^2,$$
(2)

$$G = m^2 + \left((ak)^N \cos N\phi \sin\theta + a_z k_z \cos\theta \right)^2,$$
(3)

where we have set $k_x = k\cos\phi$ and $k_y = k\sin\phi$. The gap is given by $\Delta = \sqrt{m^2 - h^2}$ at $\mathbf{k} = \mathbf{0}$ for $h < m$. As h increases the gap decreases and closes at the critical value $h = m$, as shown in Fig.1(b). Then, for $h > m$, the band splits into N Weyl points and N anti-Weyl points with the linear dispersion, as shown in Fig.1 (c). The zero-energy solutions at these $2N$ points are given by

$$ak_x = \left(h^2 - m^2 \right)^{1/2N} \cos(j\pi/N) \sin\theta,$$
(4)

$$ak_y = \left(h^2 - m^2 \right)^{1/2N} \sin(j\pi/N) \sin\theta,$$
(5)

$$a_z k_z = \pm\sqrt{h^2 - m^2} \cos\theta,$$
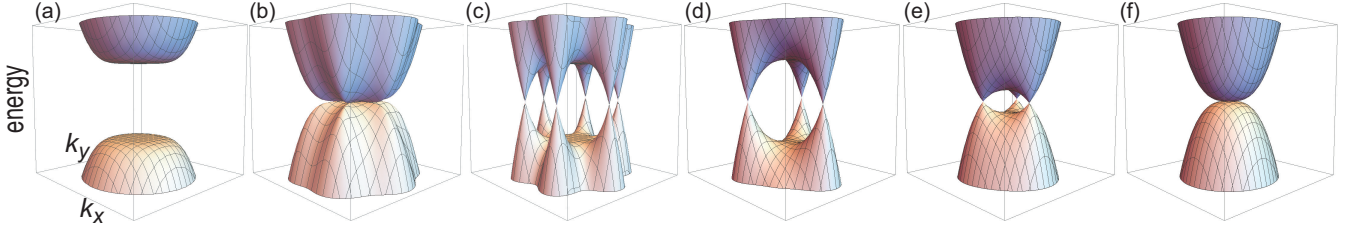(6)

with $j = 1, \cdots, 2N$.

FIG. 1: Bird's eye's views of the band structure on the $k_x k_y$ plane at $k_z = 0$ in the case of $N = 3$, when the Zeeman field is $\mathbf{h} = 0$ for (a), $\mathbf{h} = (m, 0, 0)$ for (b), and $\mathbf{h} = (2m, 0, 0)$ for (c). Three pairs of Weyl and anti-Weyl points are observed in (c). Similar views at $k_z = (\sqrt{h^2 - m^2}/a_z) \cos \theta$, when $\mathbf{h} = 2m(\cos \theta, 0, \sin \theta)$ with $\theta = \frac{1}{4}\pi$ for (d), $\theta = \frac{4}{9}\pi$ for (e), and $\theta = \frac{1}{2}\pi$ for (f). Three Weyl points are observed in (d) and (e), which are merged into one multiple-Weyl point in (f).

The Fermi surface is composed of the zero-energy points. All of them are on a single plane parallel to the $k_x k_y$ plane at k_z fixed by (6). We show the almost zero-energy surface given by $E = \delta$ for a fixed small value of δ at $h = 2m$ in Fig.2(a1) and (c1) for $N = 2$ and 3, respectively. Each of these points on the plane at $k_z > 0$ ($k_z < 0$) is a monopole (antimonopole) with the monopole charge ± 1.

This can be seen in the standard way. Namely, solving for the eigenstate $|\psi\rangle$ in the Hamiltonian (1), we calculate the Berry connection by $A_i(\mathbf{k}) = -i\langle\psi|\partial_i|\psi\rangle$ and the Berry curvature by $\mathbf{\Omega}(\mathbf{k}) = \nabla \times \mathbf{A}(\mathbf{k})$, where $\partial_i = \partial/\partial k_i$. We show the Berry curvature at $h = 2m$ in Fig.2(b1) and (d1) for $N = 2$ and 3, respectively. Each Weyl (anti-Weyl) point has a hedgehog (anti-hedgehog) structure and possess the unit (minus unit) of monopole charge in the Berry curvature. The N Weyl (anti-Weyl) points merge into one Weyl (anti-Weyl) point at $\mathbf{h} = (0, 0, h)$. The coordinate of the point is given by $(0, 0, \pm\sqrt{h^2 - m^2})$, which we call the north or south pole. We clearly see how the N hedgehog structures merge into one hedgehog structure in Fig.2. The dispersion along the k_x and k_y axes is the N-th power, which manifests that the Fermi surface is largely flattened along the k_x and k_y directions compared with the k_z direction as shown in Fig.2(a5) and (c5).

Anomalous Hall effects: It is known that a pair of Weyl points contributes to the anomalous Hall conductivity, which is proportional to the distance of the pair[3]. It is due to the fact that the system has a nontrivial Chern number as a function of k_z. We seek if similar phenomena exist in the present system.

The anomalous Hall conductance is given by $\sigma_{ij} = (e^2/\hbar)\varepsilon_{ij\ell} \int C(k_\ell) dk_\ell$, where $C(k_\ell)$ is the Chern number at k_ℓ and defined by $C(k_\ell) = \sum_\nu C_\nu(k_\ell)$ with $C_\nu(k_\ell) = (1/2\pi)\varepsilon_{\ell ij} \int dk_i dk_j \Omega_\ell(\mathbf{k})$. The summation $\sum_\nu$ runs over the occupied bands indexed by ν. Here, $C_\nu(k_\ell)$ is the total Berry magnetic flux through the $k_i k_j$ plane that comes from the band indexed by ν.

A monopole charge is given by the surface integral of the Berry magnetic flux surrounding a Weyl point. We take a cylindrical surface containing a single Weyl point whose thickness is infinitesimally small and whose radius is infinitely large. Let the vector parallel to the cylindrical axis be $(\sin\vartheta, 0, \cos\vartheta)$. We focus on the Chern number $C(k_\vartheta) = C(k_x)\sin\vartheta + C(k_z)\cos\vartheta$ with $k_\vartheta = k_x\sin\vartheta + k_z\cos\vartheta$. The contribution from the side of the cylinder is zero. The contribution from the top and bottom surfaces are the Chern

numbers $C(k_\vartheta + \delta)$ and $C(k_\vartheta - \delta)$, respectively, and hence the total contribution is $C(k_\vartheta + \delta) - C(k_\vartheta - \delta) = \pm 1$ for a monopole or an antimonopole. Since there are no monopoles and no antimonopoles as $k_\omega \to -\infty$, we set $\lim_{k_\omega \to -\infty} C(k_\vartheta) = 0$. In this way $C(k_\vartheta)$ is obtained as a function of k_ϑ.

The Chern number $C(k_z)$ is calculated as follows. For the the band with $\chi = -1$ and $\eta = -1$, we obtain explicitly as

$$C_\nu(k_z) = \begin{cases} N/2 & \text{for } a_z|k_z| > \sqrt{h^2 - m^2}\cos\theta \\ -N/2 & \text{for } a_z|k_z| < \sqrt{h^2 - m^2}\cos\theta \end{cases}. \quad (7)$$

It changes the sign at the position of the Weyl and anti-Weyl points. On the other hand, the Chern number does not change as a function of k_z for the band with $\chi = -1$ and $\eta = 1$, i.e., $C_\nu(k_z) = -N/2$. The total Chern number is given by the sum of these two contributions as

$$C(k_z) = \begin{cases} 0 & \text{for } a_z|k_z| > \sqrt{h^2 - m^2}\cos\theta \\ -N & \text{for } a_z|k_z| < \sqrt{h^2 - m^2}\cos\theta \end{cases}. \quad (8)$$

Similarly we can calculate $C(k_x)$ and $C(k_y)$.

It follows that the anomalous Hall conductance is given as

$$\sigma_{xy} = N\frac{e^2}{\pi h}\sqrt{h^2 - m^2}\cos\theta. \quad (9)$$

It is enhanced by N times compared with that in normal Weyl semimetals.

Fermi arcs: In what follows we study the case $\mathbf{h} = (0, 0, h)$. N Weyl points merge into a single multiple-Weyl point at the north or south pole for $h > m$. To such a case we apply the same argument and find that the monopole charge at the north (south pole) is $\pm N$. The system is a quantum anomalous Hall insulator for each k_z when $a_z|k_z| < \sqrt{h^2 - m^2}$. The N chiral edge modes appear at the sample edges based on the bulk-edge correspondence. Each chiral edge must cross the Fermi energy at a certain momentum[3]. These zero-energy states are present continuously between the north and south poles, implying the emergence of N Fermi arcs connecting these poles.

Multiple-Weyl fermions: In order to make a further study of the monopole, we derive the effective Hamiltonian for multiple-Weyl fermions under the Zeeman field $\mathbf{h} = (0, 0, h)$ with $h > m$. We first construct a unitary transformation
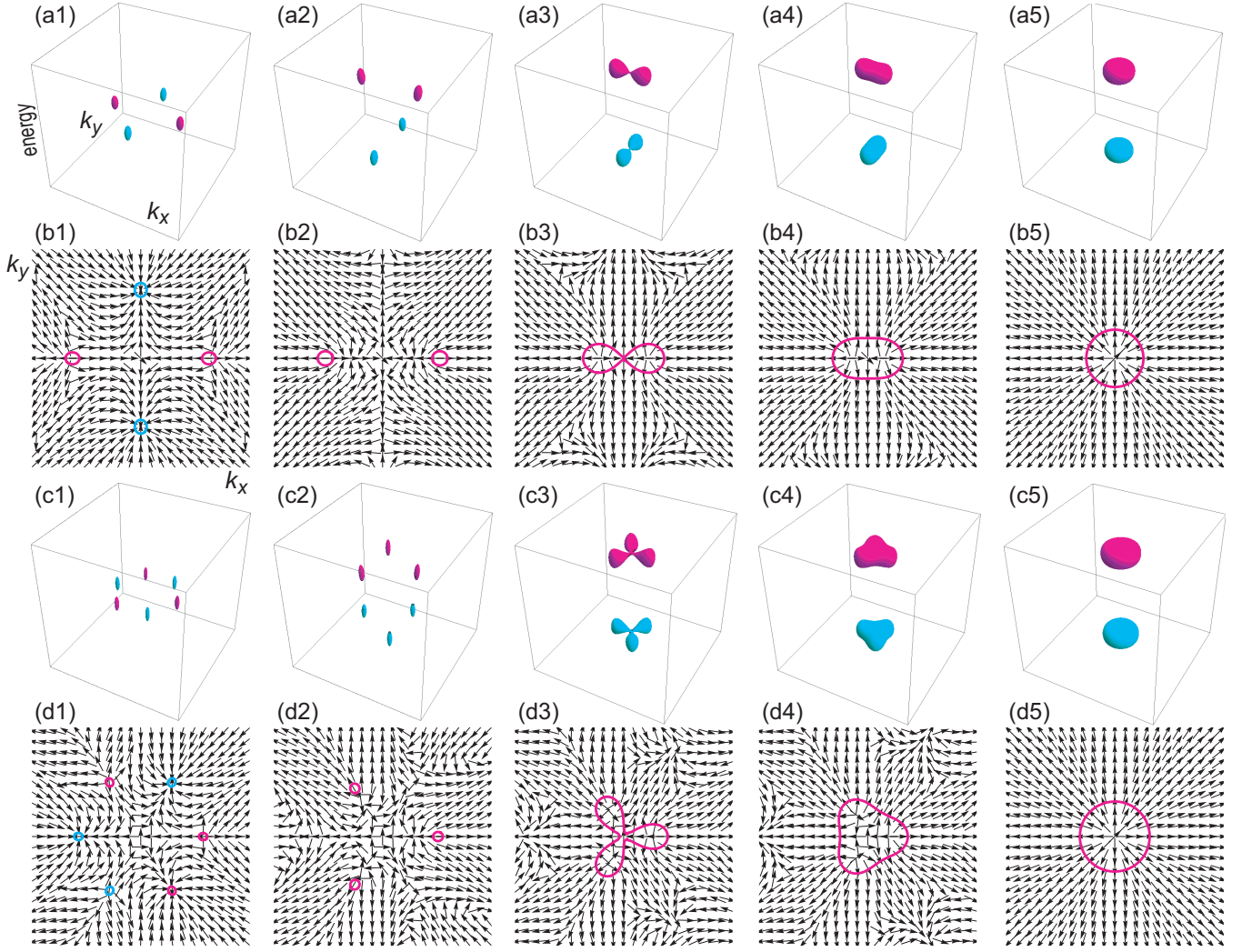
FIG. 2: Bird's eye's views of the almost zero-energy surfaces ($E = \delta$) of the Hamiltonian in the case of $N = 2$ for $\mathbf{h} = 2m(\cos\theta, 0, \sin\theta)$ with (a1) $\theta = 0$, (a2) $\theta = \frac{1}{4}\pi$, (a3) $\theta = \frac{4}{9}\pi$, (a4) $\theta = \frac{17}{36}\pi$, (a5) $\theta = \frac{1}{2}\pi$. (b1)-(b5) Normalized Berry curvature $(\Omega_x, \Omega_y)/\sqrt{\Omega_x^2 + \Omega_y^2}$ and the almost zero-energy surfaces corresponding to (a1)-(a5). Two pairs of monopoles (in magenta) and antimonopoles (in cyan) are observed in (b1), while two monopoles are observed in (b2) and (b3). They approach one another very much in (b4), and are merged into one monopole in (b5). Magenta circles become larger as θ approaches $\frac{1}{2}\pi$, indicating that the dispersion becomes flatter. (c1)-(c5) Bird's eye's view of the almost zero-energy surface of the Hamiltonian in the case of $N = 3$. The Zeeman field is the same as that of (a1)-(a5). (d1)-(d5) Normalized Berry curvature corresponding to (c1)-(c5).

U that diagonalizes the Hamiltonian $H(0, 0, k_z)$. We then transform the Hamiltonian $H(k_x, k_y, k_z)$ by the same unitary transformation U. We may extract the 2×2 matrix whose eigenvalues vanish at the north and south poles. Expanding it around $k_z = \pm\sqrt{h^2 - m^2}$, we obtain

$$H_{\text{eff}} = -a^N \left(k_+^N \sigma_- + k_-^N \sigma_+\right)$$
$$\mp \sqrt{1 - \frac{m^2}{h^2}} \left(a_z k_z \mp \sqrt{h^2 - m^2}\right) \sigma_z. \quad (10)$$

This is the effective Hamiltonian valid around the north or south pole.

We prove that the north pole has the monopole charge N. With the use of the eigenstate of the Hamiltonian (10) we may derive the Berry curvature as

$$(\Omega_x, \Omega_y, \Omega_z) = \frac{N a^{2N} a_z \left(k_x^2 + k_y^2\right)^{N-1} (k_x, k_y, N k_z)}{2 \left(a^N \left(k_x^2 + k_y^2\right)^N + a_z^2 k_z^2\right)^{3/2}}. \quad (11)$$

This describes the momentum-space monopole at the north pole. It is easy to show $\partial_i \Omega_i(\mathbf{k}) = 0$ except for $\mathbf{k} = 0$. Hence, we find $\partial_i \Omega_i = \rho\delta(\mathbf{k})$ with a constant ρ. We make a change of the variables, $k_x = (K \sin\theta)^{1/N} \cos\phi$, $k_y = (K \sin\theta)^{1/N} \sin\phi$ and $k_z = K \cos\theta$, with (K, θ, ϕ) being the polar coordinate. To determine the constant ρ, we use the Gauss theorem by choosing a sphere with radius K. We then
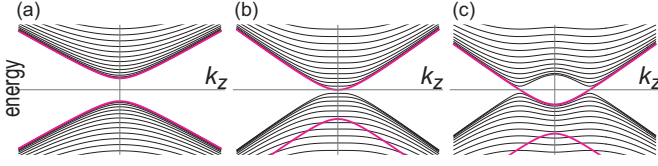
FIG. 3: Landau levels as a function of k_z. (a) $h = 0$ (below the critical value), where the edge spectrum is embedded in the bulk spectrum. (b) $h = m$ (the critical value), where a part of the edge spectrum goes away from the Fermi energy toward the bottom. (c) $h = 2m$ (above the critical value), where the chiral edge modes appear at the Weyl and the anti-Weyl points. The bulk spectrum is colored in black, while the edge spectrum is colored in magenta. The edge spectrum is N-fold degenerated.

have

$$\rho = \epsilon_{ij\ell} \oint \Omega_i dk_j dk_\ell = \frac{N}{2} \frac{1}{2\pi} \oint \sin\theta d\theta d\phi = N \quad (12)$$

after a straightforward calculation.

Magnetic field and Landau levels: We have so far introduced only the magnetization as an external parameter to control the system. As far as the emergence of multiple-Weyl points concerns, we may also introduce the magnetic field.

For definiteness, we apply the magnetic field along the z axis. Then, the cyclotron motion in the xy plane forms Landau levels[25,32,33]. As a result, the system becomes a one-dimensional system along the k_z axis. By making the minimal substitution, the Hamiltonian reads

$$\hat{H} = \tau_z \left(\hbar\omega_c \left(\hat{a}^\dagger \right)^N \sigma_- + \hbar\omega_c \hat{a}^N \sigma_+ + a_z k_z \sigma_z \right) + m\tau_x + h\sigma_z,$$
$$(13)$$

where $\hat{a}$ is the Landau-level ladder operator with $[\hat{a}, \hat{a}^\dagger] = 1$, and $\hbar\omega_c$ is the cyclotron energy. The bulk spectrum is

$$E_n^{\chi\eta} = \chi\sqrt{\frac{(n+N)!}{n!}\hbar\omega_c + \left(\sqrt{a_z^2 k_z^2 + m^2} + \eta h\right)^2}, \quad (14)$$

with the eigenstates being

$$\psi = (u_n |n\rangle, u_{n+N} |n+N\rangle, u_n |n\rangle, u_{n+N} |n+N\rangle)^t$$
$$(15)$$

for $n = 0, 1, 2, \cdots$. In addition we have N-fold degenerated Landau levels,

$$E = -h \pm \sqrt{a_z^2 k_z^2 + m^2}, \quad (16)$$

with the eigenstates being $\psi = (0, u_\nu |\nu\rangle, 0, u_\nu |\nu\rangle)^t$, where $\nu = 0, \cdots, N-1$. The gap closes at $|h| = m$. We illustrate the Landau levels as a function of k_z in Fig.3. Chiral edge modes emerge for $|h| > m$, where the degeneracy is N.

We have shown that, applying the magnetic field along the z-axis, the multiple-Weyl semimetal is created for $|h| > m$, where the chiral anomaly is enhanced by N times.

Lattice Hamiltonian: It would be interesting to construct a lattice Hamiltonian as in the case of the crossing-line nodal

semimetals[29], from which the continuum Hamiltonian (1) follows as a low energy theory. A simplest realization would be

$$H = -2^{N-1} t \tau_z \left[\sigma_x \prod_{j=1}^N \sin\left(\mathbf{d}_j^1 \cdot \mathbf{k}\right) + \sigma_y \prod_{j=1}^N \sin\left(\mathbf{d}_j^2 \cdot \mathbf{k}\right) \right]$$
$$+ t_z \sigma_z \sin a_z k_z + m\tau_x + \mathbf{h} \cdot \sigma, \quad (17)$$

with $\mathbf{d}_j^1 = a d_N^1 \left(\sin\left[(2j+1)\pi/2N\right], \cos\left[(2j+1)\pi/2N\right], 0 \right)$ with $d_1^1 = d_3^1 = 1$ and $d_2^1 = \sqrt{2}$ and $\mathbf{d}_j^2 = a d_N^2 \left(\sin\left[j\pi/N\right], \cos\left[j\pi/N\right], 0 \right)$ with $d_1^{s2} = d_2^{s2} = 1$ and $d_3^{s2} = \sqrt{3}/2$, where t, t_z are transfer energies, and a, a_z are lattice constants. The energy spectrum has the zero-energy points at the Γ point $(0, 0, 0)$. In the vicinity of the Γ point, the lattice Hamiltonian (17) is expanded and yields the continuum Hamiltonian (1).

Discussions: It is customary to apply the magnetic field in order to generate a Weyl semimetal from a Dirac semimetal. However, it creates Landau levels. As has been argued in Ref.[16], Weyl points are well separated from a Dirac point at 6 Tesla, which has experimentally been observed by the negative resistance due to the induced chiral anomaly[17–22]. Similarly we expect to have N pairs of separated Weyl points, which will eventually merge into a pair of multiple-Weyl points by controlling the magnetic field. They are observed as n gap-closing points $(2 \le n \le 2N)$ projected to the magnetic field direction. In particular, we have shown the emergence of multiple-Weyl points together with the enhanced chiral anomaly by controlling the magnetic field along the z axis with $n = 2$, which is protected by the C_N symmetry along the z axis as in Fig.3c. This phenomenon will be observed by the enhanced negative resistance.

On the other hand, in order to study a merging process of N monopoles into one monopole carrying monopole charge N, it is necessary to control the magnetization. We would argue a possible experimental study of the merging process. It has been argued[34–39] that the Zeeman field can be introduced by doping magnetic impurities. Indeed, recent experiments have demonstrated that uniform Zeeman field is realized by this way in magnetic topological insulators, where quantum anomalous Hall effects are clearly observed[40–42]. An actual method of controlling the magnitude of the magnetization is by tuning the temperature. The direction of the magnetization may be controlled by applying the magnetic field at high temperature where the system is paramagnet. By cooling the sample, the magnetization direction is fixed to be the external magnetic field direction. Once the magnetization is fixed at low temperature, we remove the magnetic field.

When the mass parameter m is large, we need a very large Zeeman field, which make it difficult to carry out any experiments on the merging process. However, our theory is valid however small m may be. Recent study shows that a cubic-Dirac semimetal is realized in quasi-one-dimensional transition-metal monochalcogenides by first-principles calculations[31], where the mass parameter is almost zero. It will be possible to realize the merging process for small m since it occurs at $h = m$. In this sense, quasi-one-dimensional transition-metal monochalcogenides will be an

ideal playground to verify the results in our predictions.

[1] M. Z. Hasan and C. L. Kane, Rev. Mod. Phys. **82**, 3045 (2010)

[2] X.-L. Qi and S.-C. Zhang, Rev. Mod. Phys. **83**, 1057 (2011)

[3] P. Hosur, X.L. Qi, C. R. Physique **14**, 857 (2013).

[4] M. Ezawa, J. Phys. Soc. Jpn. **84**, 121003 (2015).

[5] S. Murakami, New J. Phys. **9**, 356 (2007).

[6] A. A. Burkov and L. Balents, Phys. Rev. Lett. **107**, 127205 (2011).

[7] K.-Y. Yang, Y.-M. Lu, and Y. Ran, Phys. Rev. B **84**, 075129 (2011).

[8] H. B. Nielsen and M. Ninomiya, Phys. Lett. B **130**, 389 (1983).

[9] A. A. Zyuzin and A. A. Burkov, Phys. Rev. B **86**, 115133 (2012).

[10] X. Huang, L. Zhao, Y. Long, P. Wang, D. Chen, Z. Yang, H. Liang, M. Xue, H. Weng, Z. Fang, X. Dai, and G. Chen, Phys. Rev. X **5**, 031023 (2015).

[11] C.-X. Liu, P. Ye, and X.-L. Qi Phys. Rev. B **87**, 235306 (2013)

[12] C. L. Zhang, et. al Nat. Com. **7**, 10735 (2016)

[13] X. Wan, A. M. Turner, A. Vishwanath, and S. Y. Savrasov Phys. Rev. B **83**, 205101 (2011)

[14] S.Y. Xu, et.al, Science, **349**, 613 (2015)

[15] E. V. Gorbar, V. A. Miransky, I. A. Shovkovy, Phys. Rev. B 88, 165105 (2013)

[16] J. Cano, B. Bradlyn, Z. Wang, M. Hirschberger, N. P. Ong, and B. A. Bernevig, Phys. Rev. B 95, 161306(R) (2017)

[17] M. Hirschberger, S. Kushwaha, Z. Wang, Q. Gib- son, C. A. Belvin, B. A. Bernevig, R. J. Cava, and N. P. Ong, Nat. Mat. 15, 1161 (2016).

[18] C. Shekhar, A. K. Nayak, S. Singh, N. Kumar, S.-C. Wu, Y. Zhang, A. C. Komarek, E. Kampert, Y. Skourski, J. Wosnitza, W. Schnelle, A. McCollam, U. Zeitler, J. Kubler, S. S. P. Parkin, B. Yan, and C. Felser, (2016), arXiv:1604.01641.

[19] J. Xiong, S. K. Kushwaha, T. Liang, J. W. Krizan, M. Hirschberger, W. Wang, R. J. Cava, and N. P. Ong, Science 350, 413 (2015).

[20] T. Liang, Q. Gibson, M. N. Ali, M. Liu, R. Cava, and N. Ong, Nat. Mater. 14, 280 (2015).

[21] C.-Z. Li, L.-X. Wang, H. Liu, J. Wang, Z.-M. Liao, and D.-P. Yu, Nat. Comm. 6, 10137 (2015).

[22] H. Li, H. He, H.-Z. Lu, H. Zhang, H. Liu, R. Ma, Z. Fan, S.-Q. Shen, and J. Wang, Nat. Comm. 7, 10301 (2016)

[23] C. Fang, M. J. Gilbert, X. Dai, and B. A. Bernevig, Phys. Rev. Lett. **108**, 266802 (2012).

[24] B.-J. Yang and N. Nagaosa, Nat. Commun. **5**, 4898 (2014).

[25] X. Li, B. Roy and S. Das Sarma, Phys. Rev. B **94**, 195144 (2016)

[26] S.-M. Huang, S.-Y. Xu, I. Belopolski, C.-C. Lee, G. Chang, T.-R. Chang, B. Wang, N. Alidoust, G. Bian, M. Neupane, D. Sanchez, H. Zheng, H.-T. Jeng, A. Bansil, T. Neupert, H. Lin, and M. Z. Hasan, Proc. Natl. Acad. Sci. **113**, 1180 (2016)

[27] S.-K. Jian and H. Yao, Phys. Rev. B **92**, 045121 (2015)

[28] S. Ahn, E. J. Mele, and H. Min, Phys. Rev. B **95**, 161112 (2017)

[29] M. Ezawa, Phys. Rev. B **96**, 041205(R) (2017)

[30] Z. Yan and Z. Wang, Phys. Rev. B **96**, 041206(R) (2017)

[31] Q. Liu and A. Zunger, Phys. Rev. X **7**, 021019 (2017)

[32] B. Roy and J. D. Sau, Phys. Rev. B **92**, 125141 (2015).

[33] M. Ezawa, Phys. Rev. B **95**, 205201 (2017)

[34] X.-L. Qi, T. L. Hughes and S.-C. Zhang, Nature Physics 4, 273 (2008)

[35] T. Yokoyama, Y. Tanaka and N. Nagaosa, Phys. Rev. B 81, 121401(R) (2010).

[36] Z. Qiao, S.A. Yang, W. Feng, W.-K. Tse, J. Ding, Y. Yao, J. Wang, and Q. Niu, Phys. Rev. B 82, 161414R (2010).

[37] W.K. Tse, Z. Qiao, Y. Yao, A.H. MacDonald, and Q. Niu, Phys. Rev. B 83, 155447 (2011).

[38] Y. Yang, Z. Xu, L. Sheng, B. Wang, D.Y. Xing, and D.N. Sheng, Phys. Rev. Lett. 107, 066602 (2011).

[39] M. Ezawa, Phys. Rev. Lett 109, 055502 (2012)

[40] Rui Yu, Wei Zhang, H. J. Zhang, S. C. Zhang, Xi Dai, Zhong Fang, Science 329, 61 (2010)

[41] Cui-Zu Chang, Jinsong Zhang, Xiao Feng, Jie Shen, Zuocheng Zhang, Minghua Guo, Kang Li, Yunbo Ou, Pang Wei, Li-Li Wang, Zhong-Qing Ji, Yang Feng, Shuaihua Ji, Xi Chen, Jinfeng Jia, Xi Dai, Zhong Fang, Shou-Cheng Zhang, Ke He, Yayu Wang, Li Lu, Xu-Cun Ma, Qi-Kun Xu, Science 340, 167 (2013)

[42] J. G. Checkelsky, R. Yoshimi, A. Tsukazaki, K. S. Takahashi, Y. Kozuka, J. Falson, M. Kawasaki, Y. Tokura, Nature Physics 10, 731 (2014)